27
9-7-82

I-5226

UCID- 19493

EMPIRICAL ANALYSIS OF SEISMIC RECORDS FOR ELEVEN NUCLEAR TESTS AT THE NEVADA TEST SITE

MASTER

Jean L. Younker
Donald L. Springer
Eileen S. Vergino

August 9, 1982

Lawrence Livermore Laboratory

Work performed under the auspices of the U.S. Department of Energy by the Lawrence Livermore Laboratory under Contract W-7405-Eng-48.

UCID--19493

DE82 021686

ABSTRACT

Regional seismic records for eleven underground nuclear explosions were processed and analyzed (empirically) in a search for source and path related patterns in the signals. These nuclear tests were conducted between August, 1979 and April, 1980; all were located in Yucca Flat at the Nevada Test Site (NTS). The seismic signals generated by these explosions were recorded on the LLNL four-station network, located at distances of 200-400 km from the NTS.

This study represents part of a continuing effort aimed at enlarging our regional seismic database. Amplitudes were measured for consistently recorded vertical component body waves, and for vertical and transverse components of surface waves. Correlation between phase amplitudes was statistically determined, and amplitude ratios were compared for four stations for the same event, and at a single station for the complete set of events. Previous studies have shown that certain amplitude ratios are relatively unaffected by the size of the explosion but sensitive to propagation effects. For this set of events, we do not find a statistically significant change in the ratio of Pg:Lg due to different propagation paths to the four stations. We do, however, find increased variability in the amplitude measurements for the smaller events in the population considered in this study. For purposes of yield estimation and discrimination based on regional signals, it is useful to characterize the stable phases propagating from NTS to the LLNL seismic stations. A continuation of this study will be aimed at developing and maintaining our regional seismic database and placing a reasonable level of effort upon controlled "experiments" to distinguish propagation path effects from source effects.

INTRODUCTION

Empirical analysis of regional seismic signals generated by nuclear explosions is an integral part of the LLNL research efforts in support of test-ban treaty verification. Both teleseismic and regional seismic signals may be used for treaty verification purposes. However, discrimination between explosions and earthquakes, and yield estimation of suspected explosions, is most difficult for small events. Dahlman and Israelson (1977) reported that a large percentage of the events that could not be classified by screening procedures currently available also could not be detected at epicentral distances greater than 10^{0}. The LLNL regional broadband seismic network surrounding the NTS (Denny, 1977) provides the capability for developing an extensive regional database, and for investigations regarding propagation path and source effects. Locations of the seismic stations and response curves for the instruments are shown in Fig. 1.

As part of the Seismic Verification Program, regional seismic records for eleven recent nuclear explosions at the NTS were analyzed. In the first phase of the study, amplitudes for the most consistently recorded phases on the vertical and horizontal transverse components of the broadband system were measured and various amplitude ratios were calculated. Previous studies of narrowband, short-period (1 Hz) data have suggested that the ratio of the maximum Lg amplitude (on vertical or transverse components) to the maximum amplitude P phase provides a stable ratio at regional distances (Blandford, 1980); Bennett and Murphy (1980) suggested that because regional phases appear as a complex wavetrain, a simple, peak amplitude measurement may not be

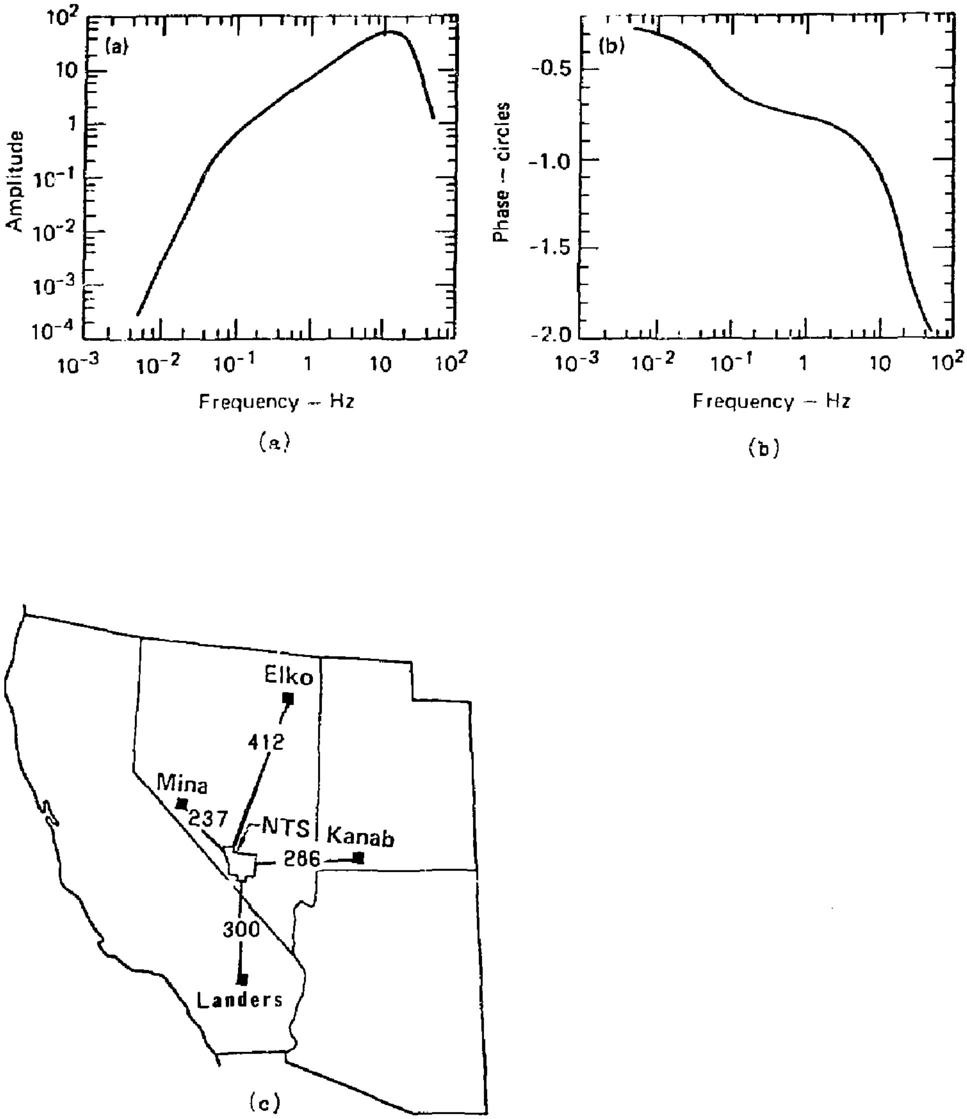

Figure 1. The amplitude transfer function for the LLNL seismic stations is displayed in (a); phase transfer function is shown in (b) (from Nakanishi, 1979); and locations of the four LLNL broadband seismic stations are shown in (c).

representative of the total energy on the regional phase. Preliminary results of this analysis of NTS explosion records support the general stability of the relationship between Lg max and Pmax.

The second part of this study was an empirical analysis of amplitude (velocity) spectra for compressional (P) waves and higher-mode surface (Lg) waves from the same eleven NTS explosions. For the compressional waves, seven separate values (three amplitude-frequency slopes, three "corner frequencies", and the "zero frequency" amplitude were estimated for those records of sufficient signal-to-noise levels to allow measurements. For the Lg wave train, three "characteristics" (moment, corner frequency and high frequency roll-off) were estimated for seven of the eleven events. Our purpose in this part of the study was to determine if some explosions produced spectral signatures which were more consistent than others. This project is aimed at assessing the factors which influence the reliability of yield estimation and discrimination. Improved understanding of variability in the NTS seismic records will improve our chances for successful interpretation of regional seismic records in other geologic settings where little is known about the source or propagation path.

PHASE I. - DATA: EMPIRICAL ANALYSIS OF BROADBAND EXPLOSION RECORDS

As part of an ongoing program for analysis of regional seismic signals generated by nuclear explosions, broadband seismic records for eleven tests conducted in Yucca Flat in 1979 and 1980 were studied. Names, dates, and approximate locations for the events are given in Table 1 and in Fig. 2.

TABLE 1. *Dates and names of nuclear explosions used in this* study. Numbers (1-11) refer to code used in tables and figures in this paper.

1	9/6/79	Hearts
2	8/3/79	Burzet
3	8/8/79	Offshore
4	4/16/80	Pyramid
5	4/3/80	Liptaur
6	8/29/79	Nessel
7	2/28/80	Tarko
8	11/29/79	Backgammon
9	3/8/80	Norbo
10	9/8/79	Pera
11	12/14/79	Azul

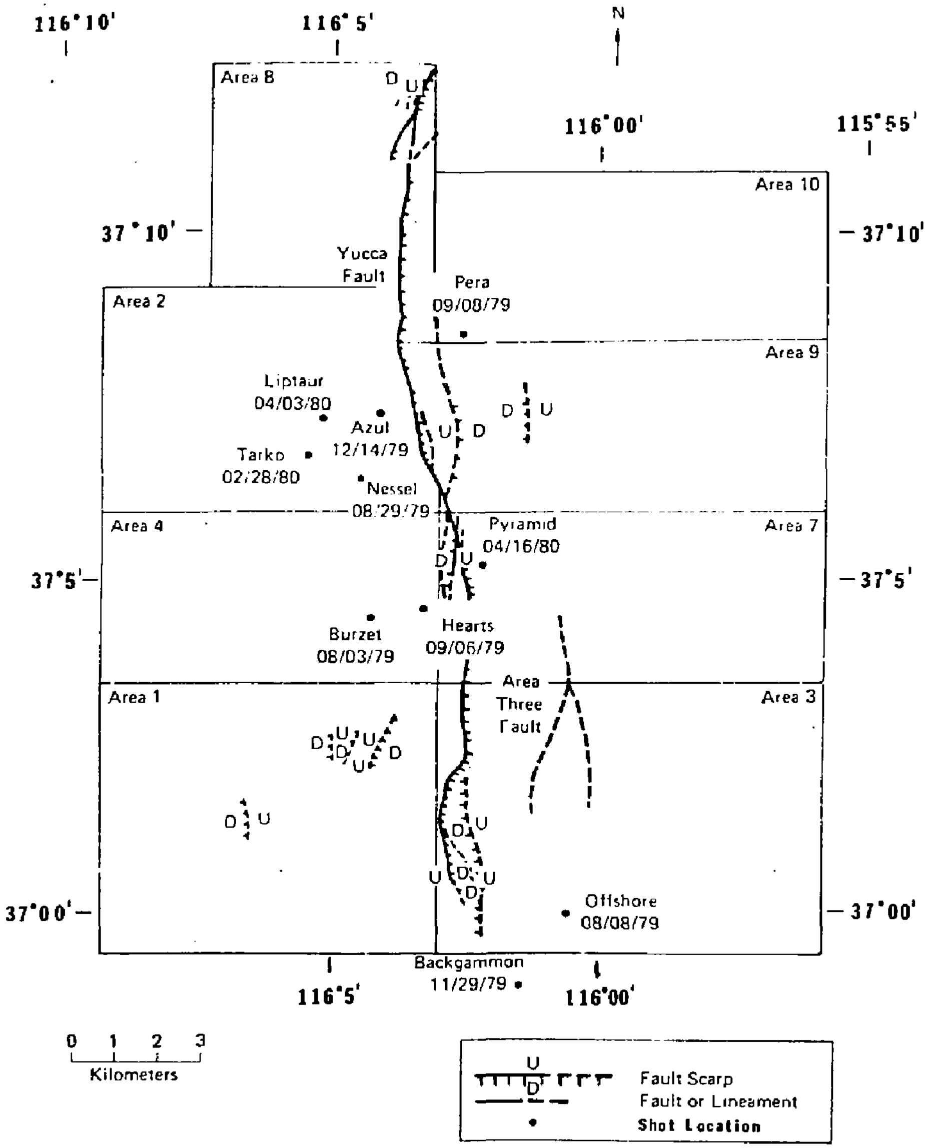

Figure 2. Yucca Flat area with locations for the eleven events (adapted from Patton and Vergino, 1981).

The main criterion for selection of seismic phases was reproducibility at a given station. Three phases appeared consistent on the vertical component, and two on the horizontal transverse component. Figure 3 is a sample record from the Mina station with the measured phases labeled. The first phase measured on the vertical component is the Pn arrival; the second is the large-amplitude, guided crustal wave, Pg. The other consistent phase on the vertical component arrives at the same time as the Lg on the horizontal component, and is thought to represent the vertical component of the Lg phase, Lg(v). The two large amplitude signals on the horizontal transverse component are probably due to multipathing, and the larger of the two amplitudes was chosen arbitrarily as the best Lg amplitude for calculation of amplitude ratios and subsequent data processing. The critically-refracted wave traveling along the top of the mantle, Pn, is the first arrival at all of the LLNL stations for NTS events. The phase labeled Pg follows the first arrival by 5 - 10 seconds at the Mina (Nevada), Kanab, (Utah), and Landers (California) stations, and by approximately 20 seconds at the Elko (Nevada) station. This phase represents the crustal compressional wave which travels with a group velocity of about 6 km/sec.

In an attempt to minimize path effects and maximize source effects, amplitudes for a given phase measured directly from broadband velocity records were averaged over the network for each explosion, with a minimum of three stations in operation. Network-averaged amplitude values for Pn, Pg, Lg(v), and Lg(t) for each explosion are shown in Table 2. Log/log plots were prepared to estimate the relative excitation of the various phases. These

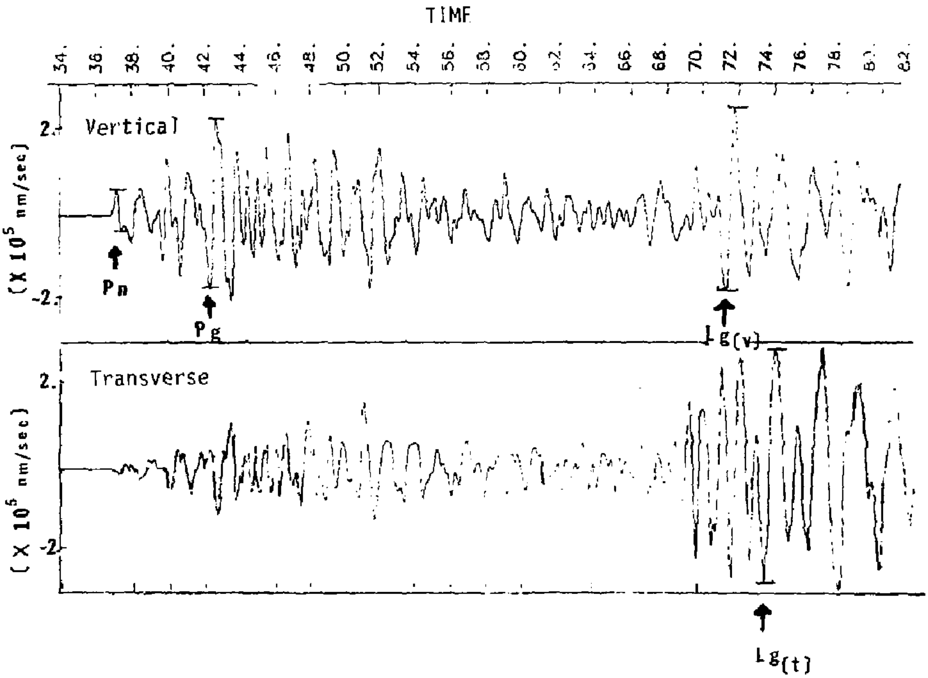

Figure 3. Mina station: broadband recording of vertical and horizontal transverse components of seismic signal generated by Hearts. Time measured in seconds after origin time; phases measured in this study are labeled on figure.

TABLE 2. Station Averages: Amplitude Data for Pg, Pn, Lg(t), Lg(v).

EVENT	NO. OF STATIONS RECORDING	Pg	Pn	Lg(t)	Lg(v)
		(10^3 nm/sec)			
1	4	316.75 (2.50)*	44.52 (1.65)	371.80 (2.57)	386.05 (2.59)
2	3	24.21 (1.38)	2.87 (.46)	44.05 (1.64)	25.42 (1.40)
3	3	27.94 (1.45)	2.44 (.38)	49.07 (1.69)	38.01 (1.58)
4	4	124.58 (2.09)	21.08 (1.32)	243.50 (2.39)	157.47 (2.20)
5	4	29.18 (2.09)	3.68 (1.32)	60.84 (2.39)	36.90 (2.20)
6	4	40.01 (1.60)	4.46 (.65)	74.58 (1.87)	56.96 (1.76)
7	3	12.77 (1.11)	3.10 (.49)	28.93 (1.46)	20.09 (1.30)
8	4	2.56 (.41)	.27 (- .57)	4.32 (.63)	2.51 (.40)
9	4	2.92 (.46)	.42 (- .38)	5.83 (.77)	3.96 (.60)
10	4	1.69 (.23)	.27 (- .57)	3.83 (.58)	2.28 (.36)
11	3	2.38 (.38)	.28 (- .55)	4.49 (.64)	4.10 (.61)

* (Log_{10} amplitudes are given in parentheses below average amplitudes)

diagrams are shown in Figures 4(a,b) and 5(a,b), and linear regression results are provided in the captions. The averaged Log Pg/Log Lg relationships show the lowest standard deviations and the best fit to a straight line, although all r^2 values are large. An r^2 (coefficient of determination) of 1.00 represents a linear relationship, or a perfect "fit" by the regression line. The greater standard deviation for Pn is probably related to measurement error because the small amplitude values for Pn were difficult to measure on the broadband seismic records used in this study. Although our data set is relatively small, an r^2 value exceeding .60 is significant at the 5% level. These relationships suggest that for Yucca Flat explosions, the ratio of surface (Lg) to body wave excitation is constant over the range of yields considered in this study.

Figure 6 provides an alternative display of the phase amplitude data in the form of amplitude ratios calculated for each event at each station. Only the Log_{10} Pg vs. Log_{10} Lg(v) is shown. Similar ratio values computed using the Lg amplitudes measured on the horizontal transverse component show greater scatter for the small events (#'s 7-11).

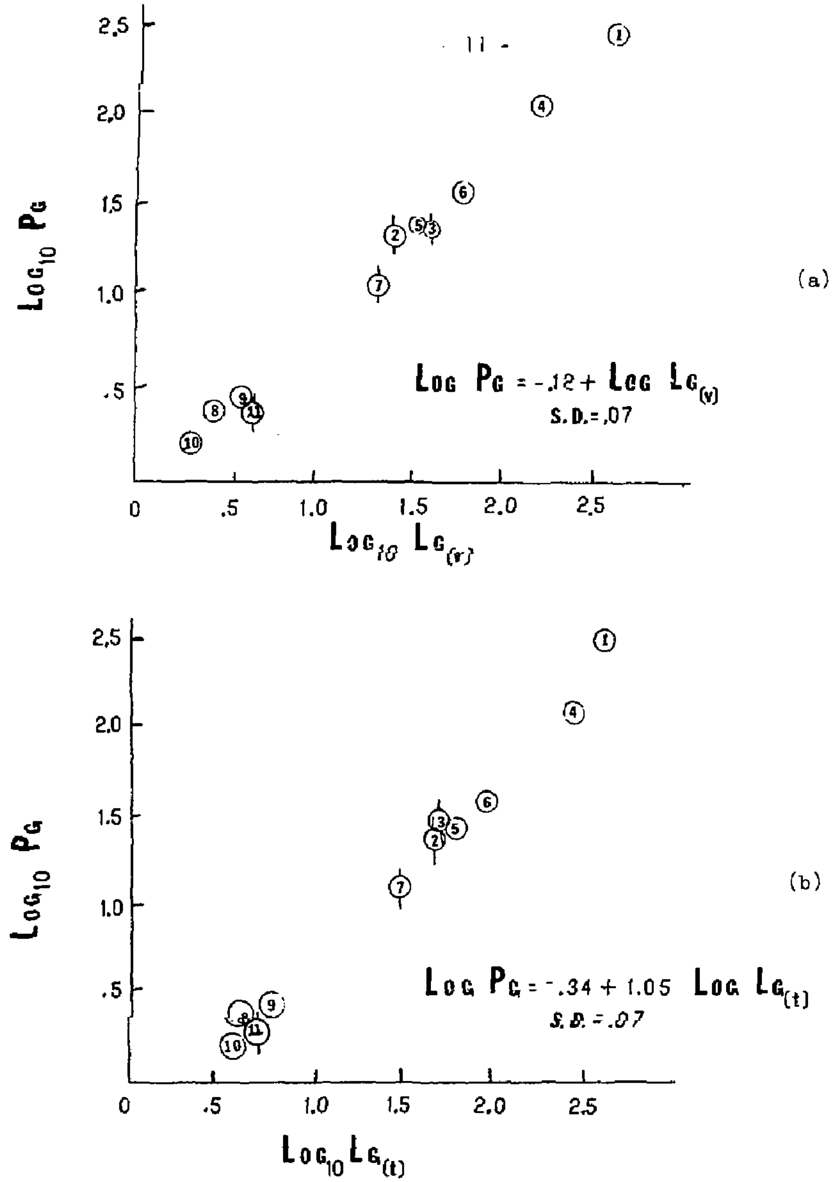

Fig. 4. Plots of Log_{10} Pg amplitudes vs. Log_{10} Lg amplitudes measured on vertical (a) and horizontal transverse (b) components. Standard deviations of the regression lines are provided for comparison. Values are averaged for 4 stations, except where Φ symbol indicates 3 stations are averaged.

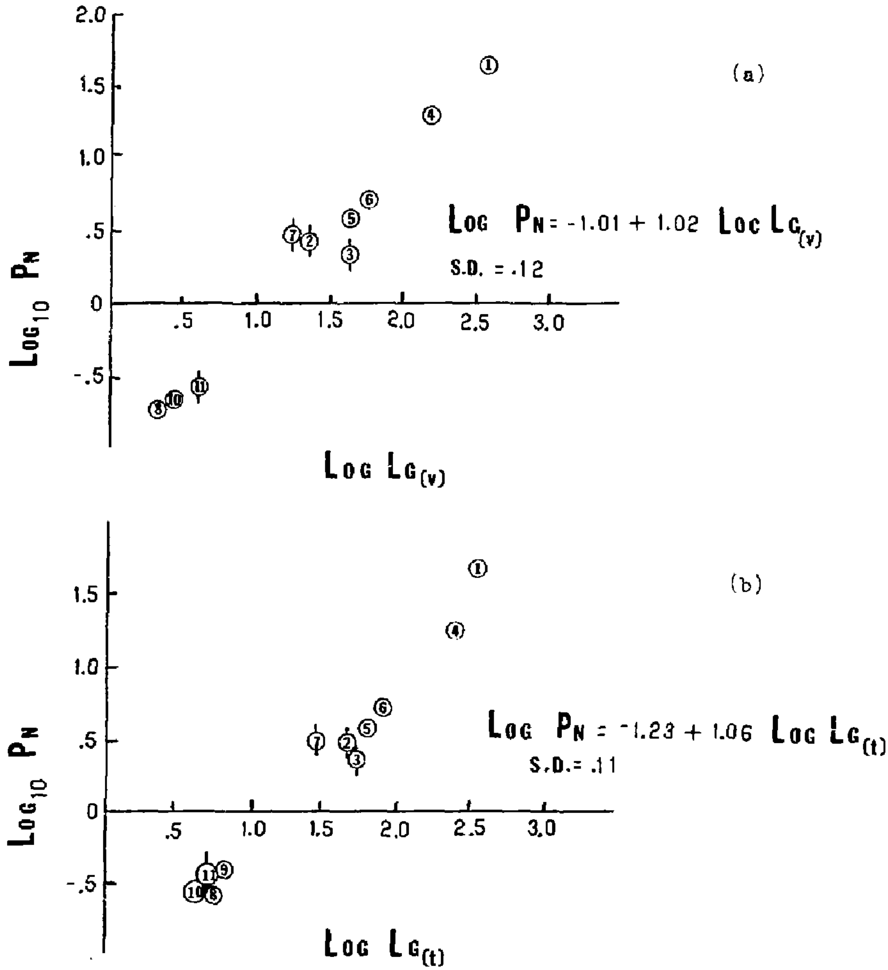

Fig. 5. Plots of Log_{10} Pn amplitudes vs. Log_{10} Lg amplitudes measured on vertical (a) and horizontal transverse (b) components.

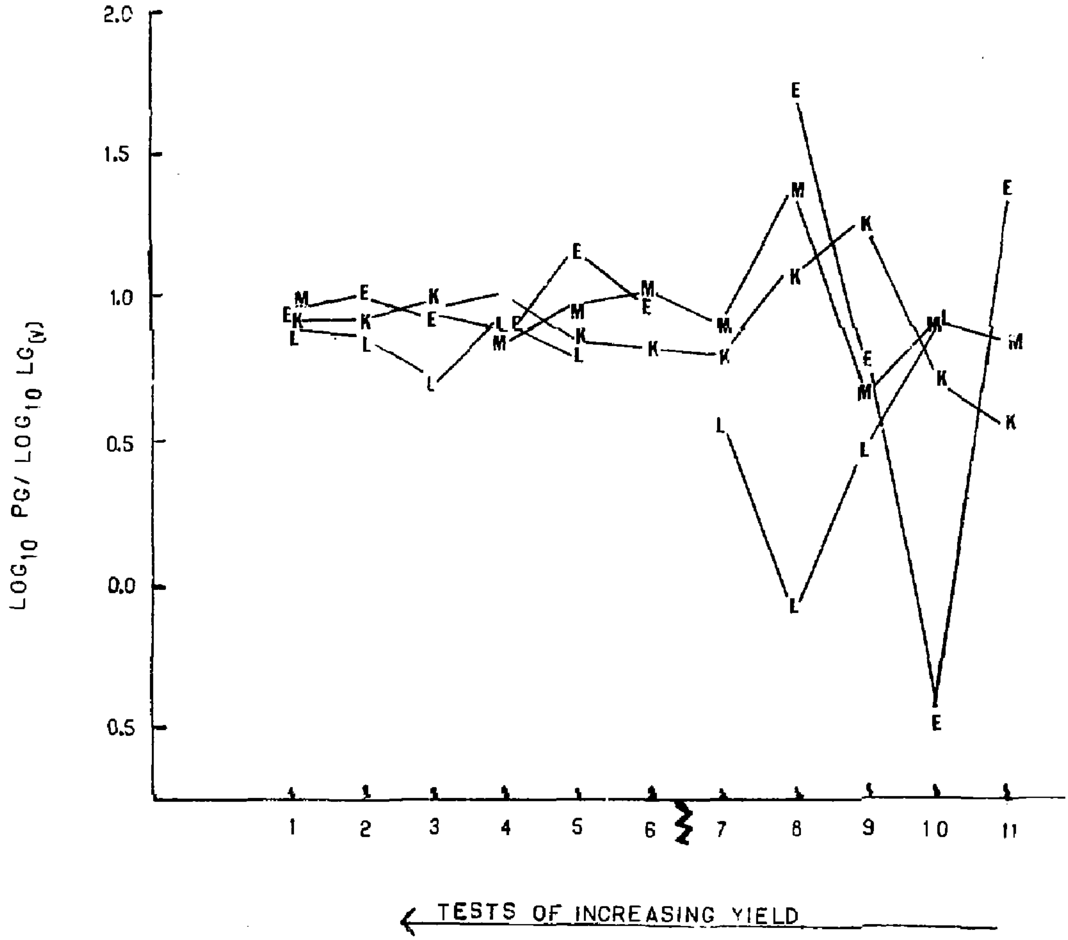

Figure 6. Amplitude ratios ($Log_{10}Pg/Log_{10}Lg(v)$ are plotted for the Yucca Flat explosions numbered 1-11 on the horizontal axis. Variability in the ratios for events #7-11 is partly due to low signal-to-noise ratios on the broadband records because these represent smaller seismic sources. Yield intervals separating explosion events #1 - 11 are not of equal size.

PHASE I. - DISCUSSION

Both the Log Pg/Log Lg and the Log Pn/Log Lg slopes show high stability for the eleven explosions when averaged over the four-station seismic network. This is in general agreement with other research on Pg/Lg amplitude ratios over regional distances (Blandford, 1980). Regression lines in Figures 4 and 5 were for station-averaged amplitude values. Regressions calculated for each station separately give the following values for the two slopes:

Log Pn/Log Lg:	Kanab	1.11 ± .03	Log Pg/Log Lg:	Kanab	1.04 ± .06
	Mina	1.03 ± .06		Mina	1.05 ± .04
	Landers	1.06 ± .06		Landers	1.07 ± .06
	Elko	.96 ± .06		Elko	1.10 ± .04

All of the above slopes are significant at the 1% level, but none of the slopes significantly differ from each other at the 5% level, based on an F-statistic which can be used to test for differences in regression coefficients (Sokal and Rohlf, 1969). The stability observed in these slopes may be, in part, due to our selection of a population of explosions that occurred in a localized source region, but it also suggests that the relative excitation of Pg and Lg is independent of the source parameters (such as yield, depth of burial, etc.) for this population.

Scatter in the amplitude ratios plotted in Fig. 6 reflects a combination of factors. Distance differences from Yucca Flat to the stations have not been taken into account, and propagation paths to the stations may be sufficiently different to cause some variability in the ratios. The striking effect is the increased scatter for the smaller tests.

PHASE II - DATA: EMPIRICAL ANALYSIS OF VELOCITY SPECTRA

Amplitude (velocity) spectra for the compressional (P) wavetrains for the set of eleven NTS explosions (Table 1) were calculated and then characterized by seven parameters. The seven values measured directly from the spectra are defined in Fig. 11. We chose to delineate three line segments because some of the Yucca events appeared to have a 2-part roll-off segment following the point of maximum frequency (f_2). Mean values and standard deviations were calculated for Φ_0, and for the three frequencies and three slopes. Although the sample size is small, the standard deviation is helpful as an indication of the dispersion about the mean. Averages for the seven parameters for compressional spectra are given in Table 4. Averages for f_1, f_2, and f_3 are fairly consistent, with the Landers station showing the most consistent data.

For seven of the events, Lg amplitude for displacement spectra from the vertical component were also calculated and characterized. The high-frequency roll-off and corner frequency for Lg were estimated in the same manner as for the compressional-wave spectra.

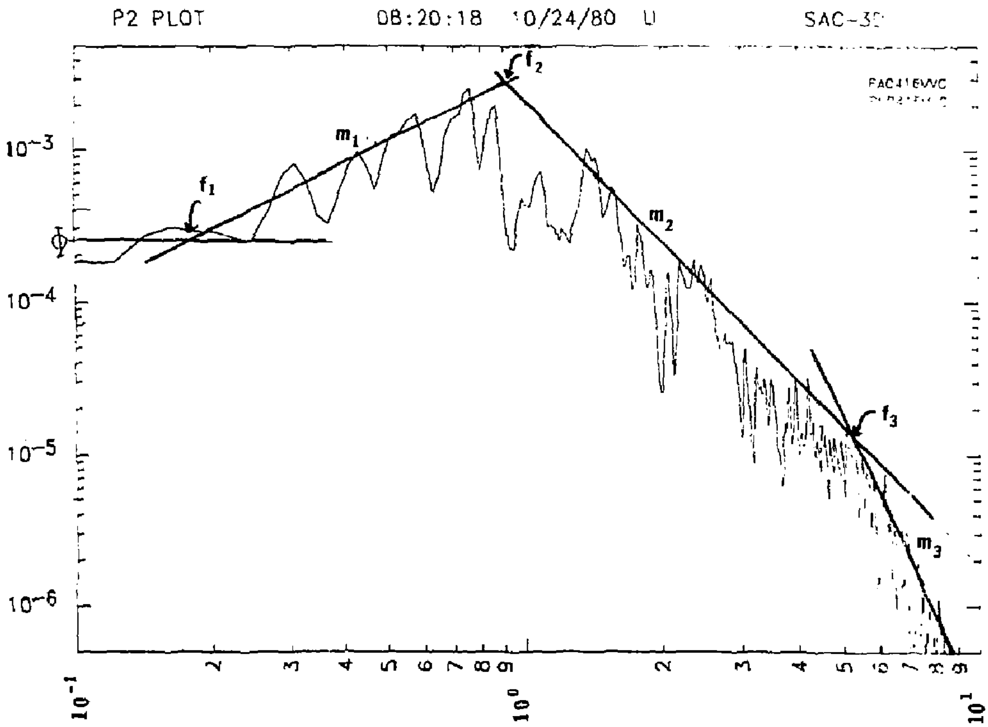

Figure 11. Velocity spectrum for the compressional wavetrain recorded at the Mina station for the event, Pyramid. The seven values used to characterize the spectrum are labeled.

TABLE 4. Averages of Amplitude Spectral Characteristics for Compressional Wavetrain.

BY STATION

	MINA	KANAB	LANDERS	ELKO
f_1	.25/.06	.22/.06	.30/.03	.26/.05
f_2	.77/.18	.71/.11	.72/.12	.67/.16
f_3	3.6/1.0	4.1/1.2	4.0/.7	3.31/.76
m_1	2.12/.79	2.24/.91	1.75/.78	2.12/1.23
m_2	-2.48/.92	-2.37/.53	-2.31/.86	-1.97/.65
m_3	-6.46/1.49	-6.13/1.23	-6.20/1.52	-6.33/1.58

BY EVENT

	Φ_o ($\times 10^{-5}$)	f_1	f_2	f_3	m_1	m_2	m_3
Hearts	62.0	.24/.07	.70/.03	4.15/1.0	1.89/.25	2.75/.18	6.21/1.15
Burzet	4.9	.30/.05	.81/.14	4.3/1.9	1.49/.36	1.8/1.0	5.54/.85
Offshore	7.7	.25/.06	.77/.16	3.4/1.0	1.07/.41	2.02/.39	5.72/1.07
Pyramid	24.7	.23/.06	.65/.18	4.3/.86	2.4/.63	2.7/.88	5.12/1.0
Liptaur	6.8	.30/.04	.57/.01	1.9/.17	3.81/.58	2.36/.27	5.1/.37
Nessel	7.50	.23/.04	.78/.13	4.2	1.75/.11	3.35/.89	6.12/.92
Tarko	2.70	–	.71/.19	2.73/.30	–	2.1/.53	4.08/.66
Backgammon	.82	–	1.0/.08	3.42/.15	–	1.76/.68	7.35/.39
Norbo	.79	–	.77/.13	4.3/.22	–	1.78/.36	7.17/.44
Pera	.57	–	.67/.10	4.15/.37	–	2.28/.50	8.57/.52
Azul	1.20	–	.60/.01	3.8/.25	–	1.79/.21	7.12/.58
Averages and Standard Deviations		.26/.06	.71/.13	3.76/.97	2.07/.91	2.28/.74	6.28/1.4

Displacement spectra for Lg were corrected for geometrical spreading and normalized to a source-receiver distance of 500 km by multiplying the entire spectrum by $\sqrt{r/500}$, where r is the source-receiver distance. The moments and high frequency roll-offs for vertical component Lg spectra are summarized in Table 5. Moments were estimated using the formulation of Street et al. (1975), where the distance-corrected, far-field displacement spectrum of the source S(w), is estimated for $r \geq r_0$ by:

$$S(w) = 4\pi\rho\beta^3 \, r_0 \, (r/r_0)^{1/2} \, \Omega \, (w)$$

where r = normalized source-receiver distance = 500 km,
ρ = density = 2.5 gm/cm^3,
β = velocity = 3.5 km/sec,
Ω (w) = observed Lg spectrum at a distance r from the source,

and

r_0 = scaling factor reflecting change in character of Lg with distance = 100 km (empirical).

The moment M_0, is then given by
S(w=0), where
Ω (w=0) $\equiv$ measured long period level.

Moments estimated by this procedure may be overestimated because the *crustal velocity chosen (β=3.5 km/sec) is high for Lg in the western U.S.* The scaling factor, r_0, is an empirical value derived for the eastern U.S., and may not be the correct value for the western U.S. However, the values presented in Table 5 were consistently derived and can be compared to each other.

Table 5. Lg (vertical component) spectral characteristics

Event - Magnitude Station*	M_o (dyne-cm)	Corner Frequency (Hz)	High Frequency Roll-off
Hearts 5.8 m_b	(x 10^{23})		
M	1.8	.76	$w^{-3.2}$
K	2.1	.76	$w^{-3.3}$
L	1.5	.60	$w^{-3.1}$
E	1.1	.65	$w^{-3.0}$
Mean	1.63 ± .37	.69 ± .07	3.15 ± .11
Nessel 4.7 m_b	(x 10^{22})		
M	1.8	1.1	$w^{-4.0}$
K	2.1	1.1	$w^{-4.2}$
L	1.2	.75	$w^{-3.1}$
E	1.2	.90	$w^{-3.5}$
Mean	1.58 ± .39	.96 ± .15	3.70 ± .43
Offshore 4.8 m_b	(x 10^{22})		
K	2.1	.95	$w^{-3.5}$
L	1.5	.70	$w^{-3.4}$
E	0.6	1.20	$w^{-4.1}$
Mean	1.4 ± .62	.95 ± .20	3.67 ± .31
Burzet 4.4 m_b	(x 10^{21})		
K	9.6	1.20	$w^{-4.0}$
L	4.5	1.00	$w^{-3.2}$
E	3.6	1.40	$w^{-4.2}$
Mean	5.90 ± 2.64	1.20 ± .16	3.80 ± .43

Table 5 (continued)

Event - Magnitude Station*		M_o (dyne-cm)	Corner Frequency (Hz)	High Frequency Roll-off
Backgammon				
		($\times 10^{21}$)		
M		0.84	1.40	$w^{-4.0}$
K		1.80	1.10	$w^{-3.8}$
L		0.60	1.40	$w^{-3.8}$
E		0.42	1.50	$w^{-4.0}$
	Mean	.91 ± .53	1.35 ± .15	3.90 ± .10
Azul 3.7 m_L				
		($\times 10^{21}$)		
M		1.2	1.0	$w^{-3.0}$
K		1.3	1.1	$w^{-3.6}$
E		0.4	1.4	$w^{-3.1}$
	Mean	.97 ± .40	1.17 ± .17	3.23 ± .26
Pera 3.6 m_L				
		($\times 10^{20}$)		
M		5.4	1.2	$w^{-2.5}$
K		5.1	1.4	$w^{-3.0}$
L		2.7	0.92	$w^{-2.5}$
E		3.0	1.50	$w^{-3.0}$
	Mean	4.05 ± 1.21	1.26 ± .22	2.75 ± .25

* M = Mina, K = Kanab, L = Landers, E = Elko

PHASE II - DISCUSSION

From a general inspection of Table 4, compressional spectra show f_1 frequency values from .2 - .3 Hz; f_2 falls between .60 and .80 Hz; and f_3 ranges from 3.0 - 5.0 Hz. The slope for m_1 varies from +1 to +3; m_2 ranges from -1.5 to -3; and m_3 ranges from -5 to -7.

There appears to be a tendency for larger explosions to have higher m_2 slopes, and for smaller explosions to have higher m_3 slopes. For small events, the value for the m_3 slope is consistently greater than four times the m_2 value, while for larger events, the m_3 value is less than twice the m_2 value. This suggests that m_2 and m_3 are more likely to represent distinctly different line segments for small events.

As predicted by scaling laws, the corner frequency increases with decreasing moment for the Lg spectra given in Table 5. This relationship occurs because corner frequency is inversely proportional to source "rise time," or yield, of the event and moment is directly proportional to yield. The moment estimates range from 2.1×10^{23} dyne-cm, recorded at Landers for the explosion Hearts, to 2.7×10^{20} dyne-cm for the explosion Pera, also at the Landers station. Corner frequencies range from .60 Hz at Landers for Hearts to 1.5 Hz for Backgammon at the Elko station. The high frequency roll-off ranges from a high of -4.2 at Elko for Burzet, to -2.5 at Mina and Landers for Pera.

Examples of the Lg spectra for the stations at Kanab and Landers are shown in Figure 12. The Kanab spectra are peaked around 0.6 Hz, while the other station spectra do not exhibit this "peaking". The moments calculated for all but one event are highest at Kanab as well. In general, the moments estimated for Mina and Kanab are at least a factor of 2 higher than the moments for Landers and Elko. Because Mina and Kanab are about 145^0 apart in azimuth, as are Landers and Elko, the difference in moment between the stations could be related to the radiation pattern of Lg, perhaps suggesting a non-isotropic generator.

It is known that large explosions generate more low frequency energy than small explosions. Because of containment concerns, we also tend to detonate large explosions more deeply. Seismic coupling is generally more efficient for deeper explosions, and we also know that there is preferential attenuation of the higher frequencies during propagation in any anelastic medium. Differences in orientation and prominence of geologic structures along propagation paths also contribute to the signal variability. The larger explosions are therefore most heavily biased toward enhancement of low frequencies, or conversely the small explosive events are biased toward a relative enhancement of the higher frequencies. However, because of the size/depth of burial relationship, the exact biases affecting a signal are difficult to determine. As our data set is enlarged, it should become possible to empirically sort out some of the quantitative relationships among these competing effects.

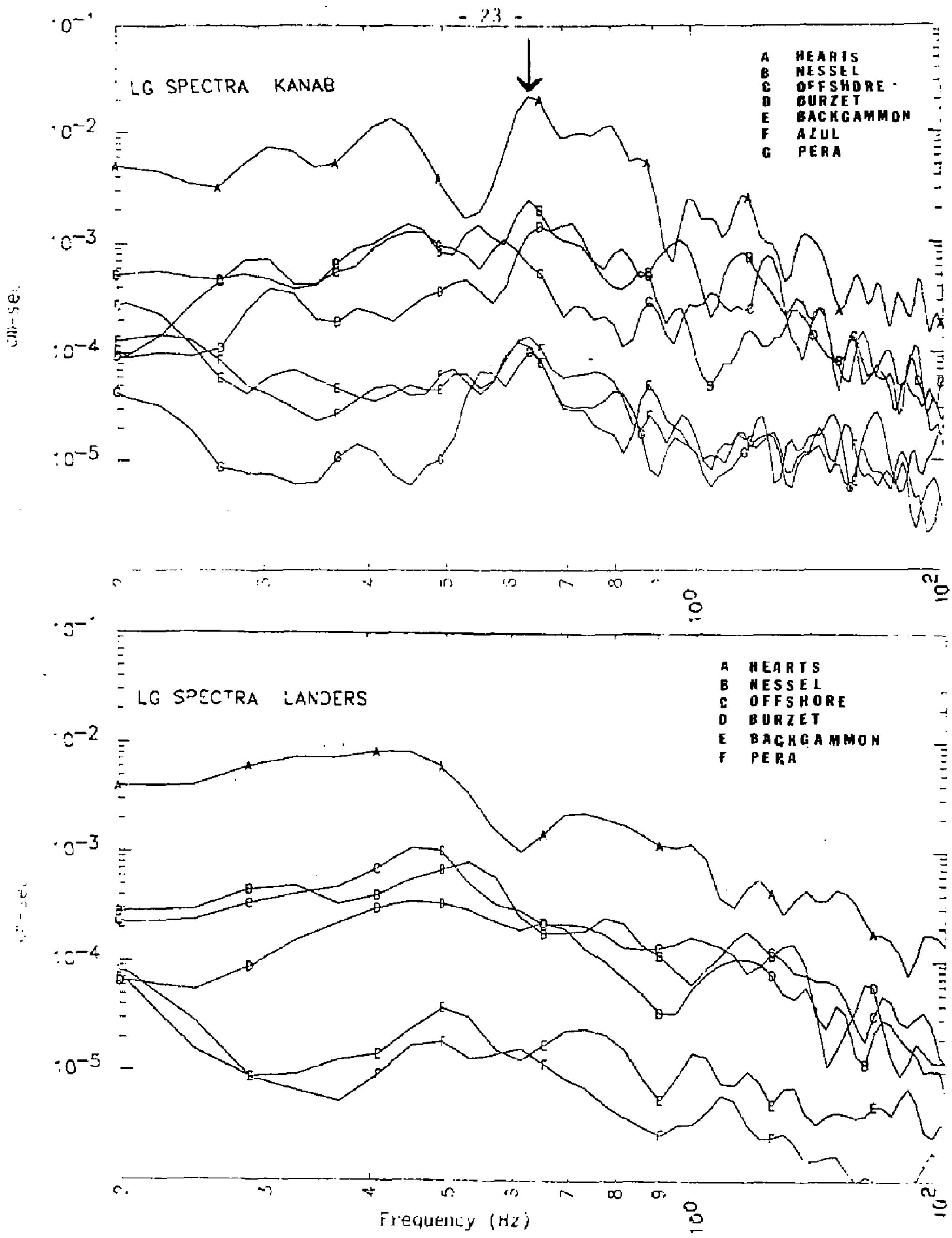

Fig. 12. Lg spectra for suite of events recorded at stations at Kanab and Landers. Note peaking of spectra at approximately .6 Hz at Kanab station.

SUMMARY

This report is a summary of an ongoing series of empirical studies of regional broadband seismic records from NTS explosions. A set of closely-spaced explosions in Yucca Flat were analyzed so that propagation effects were effectively standarized for each station. This enhances the potential for identification of source effects and for recognition of non-random near-receiver effects. Station-averaged amplitudes for Pg and Lg phases appear stable over the LLNL regional network. Slopes calculated for regressions of Pg vs Lg for each station treated separately are not significantly different at the 95% confidence level. However, there is much greater variability in the ratio for small events, probably due in part to the difficulty in accurately measuring the broadband amplitude for small events.

Amplitude spectra for compressional and Lg waves generated by the 11 explosions were calculated and analyzed. Spectral parameters were used to characterize the frequency content of the signals for comparisons between stations and between events. The Mina and Kanab stations again are similar in that moments calculated from Lg were higner by a factor of 2 than moments for Landers and Elko. This could also partly be due to the influence of the structural "grain" of the Basin and Range province. Propagation paths from the NTS to Mina and Kanab cut across the structural trends, while paths to the Elko and Landers stations are parallel to the structures. Further documentation of this effect could be useful for explaining station differences in other geological settings.

Our plans include continued development of a regional phase-amplitude database. This effort will provide the empirical basis for a more complete understanding of the propagation and generation of regional seismic phases.

ACKNOWLEDGEMENTS

The authors wish to thank the following people for their very useful reviews of this report: H. Patton, K. Nakanishi, D. Harris, S. Taylor, and P. Rodgers. We also thank Katie Young and Betty Ellison for their help in preparation of the text, and Debby Tatman for help on preparation of graphics.

REFERENCES CITED

Bennett, T. J. and J. R. Murphy, 1980, A Study of the Relative Excitation of Regional Phases for Use in Event Discrimination, Seismol. Soc. Amer. Prog. Abstr., 52nd Ann. Mtg., p. 4.

Blandford, R., 1977, Discrimination between Earthquakes and Underground Explosions, Ann. Rev. Earth Planet Sci., 5, p. 111-122.

Blandford, R., 1980, Discrimination Problems at Regional Distances, NATO Advanced Study Institute Proceedings, Identification of Seismic Sources.

Dahlman, O. and H. Israelson, 1977, Monitoring Underground Nuclear Explosions, Elsevier Sci. Publ. Co., Amsterdam, 440 pp.

Denny, M., 1977, The Installation of Horizontal Seismometers in the LLNL Seismic Network and their Calibration, UCRL Tech. Rept. 52216.

Nakanishi, K., 1979, Computer Code for the Transfer Function, UCID Tech. Rept. 18071

Patton, H. J. and E. S. Vergino, 1981, Source Effects of Surface Waves from NTS Explosions, in press, UCRL.

Sokal, R. R. and F. J. Rohlf, 1969, Biometry, Freeman, 776 p.

Street R. L., Herrman L., Nuttli O. W., 1975, Spectra Characteristics of the Lg Wave Generated by Central United States Earthquakes, Geophys. Jour. Roy. Astr. Soc. 4[illegible], p 51-63.

DISCLAIMER

Printed in the United States of America
Available from
National Technical Information Service
U.S. Department of Commerce
5285 Port Royal Road
Springfield, VA 22161
Price: Printed Copy $; Microfiche $3.50

Page Range	Domestic Price	Page Range	Domestic Price
001-025	$ 5.00	326-350	$ 18.00
026-050	6.00	351-375	19.00
051-075	7.00	376-400	20.00
076-100	8.00	401-425	21.00
101-125	9.00	426-450	22.00
126-150	10.00	451-475	23.00
151-175	11.00	476-500	24.00
176-200	12.00	501-525	25.00
201-225	13.00	526-550	26.00
226-250	14.00	551-525	27.00
251-275	15.00	526-550	28.00
276-300	16.00	601-up[1]	
301-325	17.00		

[1] Add 2.00 for each additional 25 page increment from 601 pages up.